Local Order between Chain Segments in the Glassy Polycarbonate of 2,2-Bis(4-hydroxyphenyl)propane from ^{13}C Polarization-Transfer NMR

P. Robyr,*,† Z. Gan,‡ and U. W. Suter†

Departement Werkstoffe, Institut für Polymere and Laboratorium für Physikalische Chemie, ETH-Zürich, CH-8092 Zurich, Switzerland

Received March 23, 1998; Revised Manuscript Received June 22, 1998

ABSTRACT: The local orientational order between phenylene groups and between carbonate groups in the glassy polycarbonate of 2,2-bis(4-hydroxyphenyl)propane (bisphenol-A) has been studied using ^{13}C polarization-transfer NMR under slow magic-angle sample spinning. Preferred orientations between neighboring groups have been determined from the rate constant of polarization transfer, measured as a function of the resonance frequencies in two-dimensional experiments. Nearest neighbor phenylene groups tend to have small angles between their longitudinal axes. Nearest neighbor carbonate groups can have parallel and perpendicular directions defined by the pairs of ether oxygens in each group. The perpendicular arrangements are incompatible with existing models of locally parallel chains. The packing characteristics unraveled by NMR are also compared to those of atomistically detailed simulations of bisphenol-A polycarbonate. The atomistic simulations do not reproduce well the local order measured between phenylene groups. However, they account for the occurrence of parallel and perpendicular chain segments with close carbonate groups.

1. Introduction

Much effort has been made in order to understand the relationship between the molecular structure and the macroscopic mechanical properties of amorphous polymers. This question has been repeatedly addressed by investigating local order and molecular dynamics in the glassy polycarbonate of 2,2-bis(4-hydroxyphenyl)-propane (bisphenol-A polycarbonate), hereafter simply referred to as polycarbonate. Several techniques, including dielectric relaxation, dynamic mechanical relaxation, nuclear magnetic resonance (NMR), and computer simulations have been used to study molecular motion in polycarbonate. Investigations of molecular order in polycarbonate are less numerous. Henrichs and Nicely[1] presented evidence obtained from NMR for a single preferred conformation between the isopropylidene and the phenylene groups in polycarbonate. Recently, two-dimensional NMR spectroscopy was used to characterize the chain conformation near the carbonate groups.[2,3] Some studies focused on the packing of chain segments.[4−11] Most of these investigations[4−10] favor a structural model for glassy polycarbonate in which the polymer chains are locally parallel and form so-called "bundles".[9,10] However, Lamers and coworkers[11] showed that the neutron-scattering data[4,5] could be explained without requiring parallel packing of the chain segments.

Polarization-transfer NMR spectroscopy in static samples is well-suited to study local order.[12] Since the rate constant of polarization transfer scales as the inverse sixth power of the distance between the spins,[13,14] the structure is probed on the length scale of the nearest nuclei whose type can be selected by isotopic labeling. In static samples the resonance frequency of a spin depends on the orientation of its chemical-shielding-anisotropy (CSA) tensor with respect to the static magnetic field. As the CSA tensors often have a well-characterized orientation with respect to the molecular frame,[15,16] the rate constant of polarization transfer measured as a function of the resonance frequencies in two-dimensional NMR experiments provides information on the distance between molecular fragments with different relative orientations.[12]

The rate constant of polarization transfer depends not only on the internuclear distance but also on the difference in resonance frequencies and on the angle between the internuclear vector and the static magnetic field.[12−14] These additional dependences can mask the effect of the distance and thus hinder investigation of local order.[12] Two polarization-transfer techniques were developed to easily access the structural information contained in the distance dependence of the rate constant. In radio-frequency-driven polarization transfer, the influence of the resonance-frequency difference is widely suppressed.[12,17,18] More recently, polarization transfer under slow magic-angle sample spinning (S-MAS) was introduced.[19] For spins with equal isotropic chemical shifts, this technique provides rate constants whose variations as a function of the resonance frequencies directly reveal different mean distances between molecular fragments with different relative orientations.[20]

In this contribution, we investigate the local orientational order between phenylene groups and between carbonate groups in amorphous polycarbonate using two-dimensional S-MAS polarization-transfer NMR spectroscopy in selectively ^{13}C-labeled polymers. We present polarization-transfer rate constants, measured as a function of the resonance frequencies, between phenylene carbons bonded to the carbonate groups and between carbonate carbons. The variations of the rate constants are discussed in terms of local order in three different ways. First, simple and plausible distribution functions of the relative orientation between two groups are extracted from fits to the experimental data. Second, the experimental rate constants are compared to rate constants calculated from atomistically detailed

† Departement Werkstoffe, Institut für Polymere.
‡ Laboratorium für Physikalische Chemie.

S0024-9297(98)00447-1 CCC: $15.00
Published on Web 08/19/1998

simulations. Third, the compatibility of our experimental results with the "bundle" model[9] is considered.

2. NMR Background

Polarization transfer from a group of spins A, with resonance frequencies between ω_A and $\omega_A + d\omega_A$, to a group of spins B, with resonance frequencies between ω_B and $\omega_B + d\omega_B$, can be measured using two-dimensional NMR. If the polarization transfer between each pair of spins can be described by a rate constant, polarization transfer between the two groups of spins can also be quantified, in the initial rate regime, by a rate constant. It was shown that the rate constant $R(\omega_A,\omega_B)$ with which the intensity at (ω_A, ω_B) in the 2D spectrum grows toward its quasiequilibrium value is[12]

$$R(\omega_A,\omega_B) = \frac{N}{n_A n_B} \sum_{i \in A} \sum_{j \in B} W_{ij} \tag{1}$$

where N is the total number of spins, n_A and n_B are the number of spins that belong to group A and group B, and W_{ij} is the rate constant of polarization transfer between spin i and spin j. The double sum in eq 1 runs over the $n_A \times n_B$ pairs (i, j), with spin i belonging to group A and spin j to group B.

In 2D polarization-transfer experiments under S-MAS, the evolution and detection periods are much shorter than the duration of a rotor cycle and their beginnings occur at the same position of the rotor.[19] Consequently, along both axes of the 2D spectrum, the measured frequencies correspond to those in a static sample. In contrast, the mixing period, during which polarization transfer occurs, lasts for a few rotor cycles, so that the measured rate constants are averaged over the rotation about an axis at magic angle with respect to the static magnetic field. For spins with equal isotropic chemical shifts, the averaged rate constant $\bar{R}$ is well-approximated by[20]

$$\bar{R}(\omega_A,\omega_B) = \frac{\pi}{10}\left(\frac{\mu_0 \gamma_S^2 h}{4\pi}\right)^2 \overline{\langle F_{ij}(0)\rangle}_{AB} \frac{N}{n_A n_B} \sum_{i \in A} \sum_{j \in B} \frac{1}{r_{ij}^6} \tag{2}$$

where γ_S is the gyromagnetic ratio of the spins and r_{ij} the distance between spin i and spin j. The mean intensity of the zero-quantum spectrum, $\overline{\langle F_{ij}(0)\rangle}_{AB}$, is evaluated by averaging the static values over one rotor period.[19] Usually, $\overline{\langle F_{ij}(0)\rangle}_{AB}$ hardly depends on the resonance frequencies ω_A and ω_B. From the evaluated zero-quantum intensity and the measured rate constant $\bar{R}$, the distance factor

$$f_d(\omega_A,\omega_B) = \frac{N}{n_A n_B} \sum_{i \in A} \sum_{j \in B} \frac{1}{r_{ij}^6} \tag{3}$$

can be obtained. The distance factor can also be written as

$$f_d(\omega_A,\omega_B) = \frac{1}{x_B}\int_0^\infty N_{AB}(r) r^{-6}\, dr = \frac{1}{x_A}\int_0^\infty N_{BA}(r) r^{-6}\, dr \tag{4}$$

where $N_{AB}(r)\, dr$ is the mean number of B spins at a distance between r and $r + dr$ from an A spin, and $N_{BA}(r)\, dr$ is the mean number of A spins at a distance between r and $r + dr$ from a B spin; $x_A = n_A/N$ and $x_B = n_B/N$. In the absence of local orientational order, $N_{AB}(r)/x_B$ (or $N_{BA}(r)/x_A$) is equal for all pairs of resonance frequencies ω_A and ω_B, and so is the distance factor f_d. Conversely, variations of the distance factor as a function of ω_A and ω_B reveal local order.

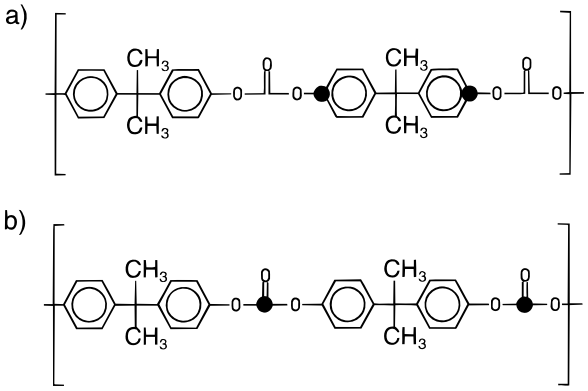

Figure 1. Repeat units of the two ^{13}C-labeled bisphenol-A polycarbonates used in this study. The black dots indicate the positions of the ^{13}C-labeled carbons (^{13}C > 99%).

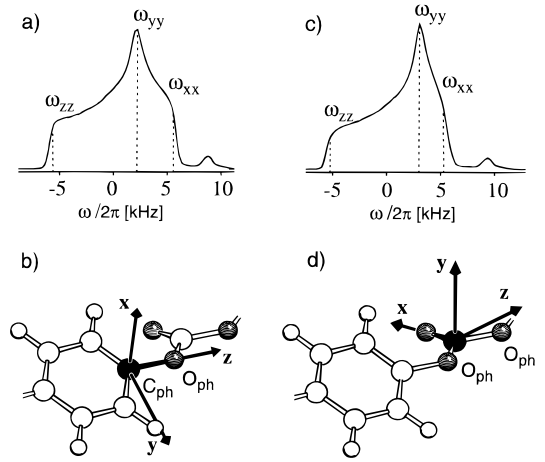

Figure 2. (a) ^{13}C NMR spectrum at 298 K of bisphenol-A polycarbonate ^{13}C-labeled at half of the phenylene carbons connected to a carbonate group (Figure 1a). The resonance frequencies corresponding to the principal values of the chemical-shielding-anisotropy tensor are indicated. (b) Orientation of the principal axes of the chemical-shielding-anisotropy tensor of the labeled carbon in the phenylene group with respect to the molecular frame. The x axis of the tensor is perpendicular to the phenylene plane and the z axis is along the bond between the phenylene and the carbonate groups. (c) ^{13}C NMR spectrum at 298 K of bisphenol-A polycarbonate with ^{13}C-enriched carbonate groups. The resonance frequencies corresponding to the principal values of the chemical-shielding-anisotropy tensor are indicated. (d) Orientation of the principal axes of the chemical-shielding-anisotropy tensor of the carbonate carbon with respect to the molecular frame. The x axis of the tensor is aligned with the C=O double bond and the z axis is parallel to the direction defined by the two ether oxygen atoms.

3. Experimental Section

Two samples of bisphenol-A polycarbonate, selectively enriched with ^{13}C (>99%), were used in this study. In one polymer, every second bisphenol-A unit is enriched with ^{13}C at the two phenylene carbons directly connected to a carbonate group (Figure 1a). In the order polymer, all carbonate carbons are enriched (Figure 1b). The one-dimensional ^{13}C spectra of the two labeled polymers are shown in Figure 2. The synthesis and the detailed characterization of the two polymers are given elsewhere;[2] here it suffices to note that the molecular weight

of the phenylene-labeled polymer is $M_w = 31\,700$ and that of the carbonate-labeled polymer is $M_w = 30\,500$; both polymers have $M_w/M_n = 1.5$.

All NMR measurements were carried out at 298 K on a home-built spectrometer working at a proton frequency of 300 MHz using a Chemagnetics (Fort Collins, CO) 6 mm double resonance MAS probe. The rf fields on the ^{13}C and the ^{1}H channels were both matched at 62 kHz. The MAS frequency was 25 ± 0.5 Hz. The 2D S-MAS polarization-transfer experiments follow the general scheme of 2D exchange spectroscopy.[19,21] Carbon coherences are prepared by cross-polarization from the protons. They freely precess during the evolution period under proton decoupling. Then, polarization transfer takes place during the mixing time, where one component of the transverse magnetization is stored along the static magnetic field for transfer under S-MAS. Finally, the carbon coherences are detected under proton decoupling. The rf pulses and the sample rotation are synchronized so that the beginnings of evolution and detection occur at the same rotor position. The polarization-transfer rate constants were obtained from a fit of a straight line to the off-diagonal intensities in the initial-rate regime, scaled by the respective intensities of the quasiequilibrium spectrum. For both polymers, seven 2D polarization-transfer experiments were used with mixing times increasing from 40 to 280 ms in 40 ms steps. Longitudinal relaxation during the mixing time was negligible. The rate constants measured in the phenylene-labeled and the carbonate-labeled polycarbonates are shown in parts a and d of Figure 3, respectively.

Additional 2D exchange experiments with proton decoupling during the mixing time were carried out without sample spinning. In these experiments, polarization transfer is quenched so that the presence of intensity in the off-diagonal region indicates reorientation processes of the labeled groups on the millisecond time scale. For both polycarbonates, static experiments at 298 K with $\gamma_H B_{1H}/(2\pi) = 40$ kHz and a mixing time of 200 ms do not show any off-diagonal intensity. Therefore, motional contributions to the rate constants of Figure 3 cumulatively exceeding 5% of the measured values can be ruled out.

4. Results and Discussion

4.I. Experimental Distance Factors. In order to obtain the distance factors from the rate constants of Figure 3, the zero-quantum intensities $\langle\overline{F_{ij}(0)}\rangle_{AB}$ need to be evaluated. These intensities were calculated, as described in ref 19, from the 2D separated-local-field spectra[22] measured in the two polycarbonate samples. The value of $\langle\overline{F_{ij}(0)}\rangle_{AB}$ scarcely varies as a function of the resonance frequencies ω_A and ω_B. The maximal deviation from the corresponding mean value is 4% for the phenylene-labeled polycarbonate and 5% for the carbonate-labeled polycarbonate. Therefore, the variations of the distance factors shown in Figure 3b,e are very similar to the variations of the corresponding rate constants.

A question that arises when considering the distance factors, or the rate constants, is to which extent does polarization transfer between two labeled carbons positioned sequentially along one chain contribute to the measured values. The distance between two phenylene-labeled carbons on both sides of the same diphenyl unit is about 7 Å and varies little because of the stiffness of the unit. The rate constant of polarization transfer between these two nuclei can be estimated to be about 0.15 s^{-1}. This is 1 order of magnitude less than the measured values and commensurate with the experimental error. Therefore, transfer between direct neighbors along one chain does not contribute significantly to the rate constants measured in the phenylene-labeled polymer. In the polymer labeled at the carbonate groups, the distance between two labeled carbons next along the chain is larger than 8 Å,[23] so the same conclusion applies. In both selectively labeled polymers, the distance factors are contributed to by pairs of carbons whose distance is less than 7 Å. The neighboring carbons belong either to different chains or to noncontiguous monomer units of the same chain, which folds back on itself.

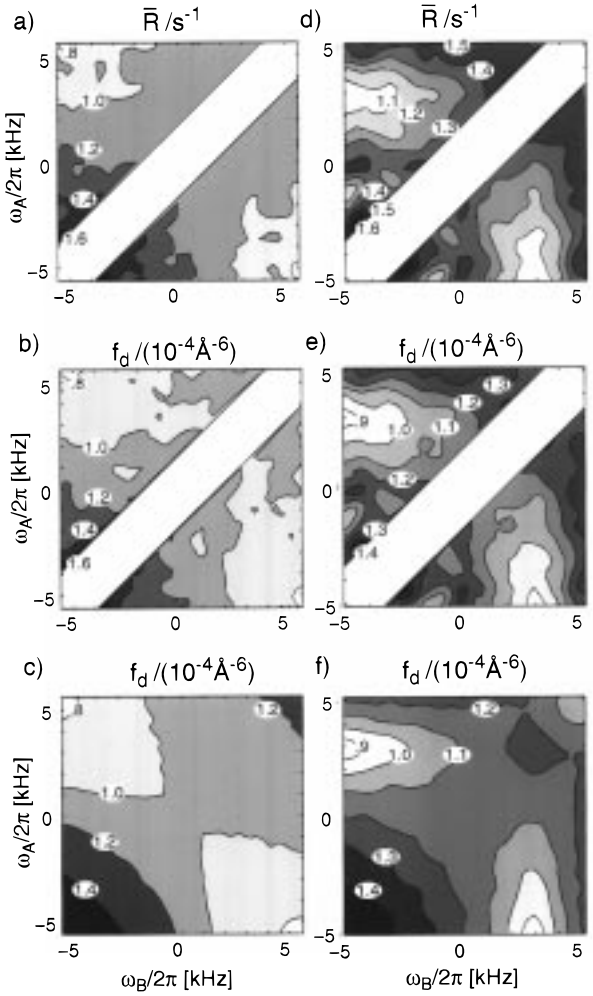

Figure 3. Polarization-transfer rate constants measured under slow magic-angle sample spinning, $\bar{R}$, and distance factors f_d at 298 K as a function of the resonance frequencies ω_A and ω_B in specifically ^{13}C-labeled bisphenol-A polycarbonates. (a) Polarization-transfer rate constant of the off-diagonal region measured in the phenylene-labeled polycarbonate shown in Figure 1a. (b) Distance factor obtained from the rate constant in part a. (c) Calculated distance factor obtained from a least squares fit to the factor in part b. (d) Polarization-transfer rate constant of the off-diagonal region measured in the carbonate-labeled polycarbonate shown in Figure 1b. (e) Distance factor obtained from the rate constant in part d. (f) Calculated distance factor obtained from a least squares fit to the factor in part e.

The distance between carbonate carbons in polycarbonate was investigated by Klug et al.[9] They interpreted their NMR measurements with a model consisting of one carbon atom coupled to two neighbors, both at a distance of 5.8 Å. Using the same model, one obtains from eq 3 for $f_d = 1 \times 10^{-4}$ Å^{-6} a distance of 5.6 Å between the central atom and the two neighbors. This distance compares well with that measured previously.[9]

4.II. Simple Interpretation of the Distance Factors. The interpretation of the distance factors f_d in

terms of local order requires the knowledge of the principal values of the CSA tensors and of the tensor orientations in the local molecular frames. The principal values of the CSA in the two polymers used in this study have already been determined.[2] It was found that $\delta_{xx} = 79$ ppm, $\delta_{yy} = 126$ ppm, and $\delta_{zz} = 230$ ppm, for the labeled carbon in the phenylene group, and that $\delta_{xx} = 90$ ppm, $\delta_{yy} = 120$ ppm, and $\delta_{zz} = 231$ ppm, for the carbonate carbon. All values are given with respect to TMS. From studies on low molecular weight crystalline compounds, rules for the orientation of the CSA tensors have been established.[15,16] For the labeled carbon in the phenylene group, the most shielded axis, *x*, is perpendicular to the aromatic plane and the least shielded axis, *z*, parallel to the $C_{ph}-O_{ph}$ bond (Figure 2b). Recently, it was found that in crystalline diphenyl carbonate, the most shielded axis of the CSA tensor of the carbonate carbon, *x*, is aligned with the C=O double bond and that the intermediately shielded axis, *y*, is perpendicular to the carbonate plane[24] (Figure 2d). This orientation is an intrinsic property of the diphenyl−carbonate fragment which also applies to polycarbonate.[24] In amorphous systems, however, small deviations (±10°) from these orientations may occur.[16,24] Such deviations would not influence significantly the conclusions drawn from this work.

The phenylene and the carbonate groups undergo at room temperature reorientational processes faster than 10 kHz.[25−29] Although these motions lead to averaged CSA tensors, the one-dimensional ^{13}C spectra at 50, 135, and 298 K of the labeled polymers used in this study differ little.[2] This stability corroborates the view that the dominant motion of the phenylene groups consists of 180° ring flips about the $C_{ph}-O_{ph}$ bond[25−28] and that the carbonate groups move about the $O_{ph}-O_{ph}$ direction.[29] Since both motions are about a principal axis of the CSA tensors of the static structures, it is reasonable to assume that the orientations of the CSA tensors with respect to the average molecular structures are the same as those in the absence of motion.

The distance factor f_d obtained from the phenylene-labeled polymer is shown in Figure 3b. It has a maximum in the region where $\omega_A \approx \omega_B \approx \omega_{zz}$ and steadily decreases along the line $\omega_A = \omega_{zz}$. Since the resonance frequency ω_{zz} corresponds to an unequivocal orientation of the CSA with respect to the static magnetic field, the spin pairs that contribute to the distance factor in the region $\omega_A \approx \omega_B \approx \omega_{zz}$ belong to neighboring phenylene groups with nearly parallel $C_{ph}-O_{ph}$ directions. In the region $\omega_A = \omega_{zz}$ and $\omega_{yy} \leq \omega_B \leq \omega_{xx}$, the two $C_{ph}-O_{ph}$ directions are nearly perpendicular. For this type of orientation, the mean distance between two labeled carbons is smaller than that for nearly aligned $C_{ph}-O_{ph}$ directions. Further, the hardly significant variation of the distance factor along the line $\omega_A = \omega_{xx}$ indicates that neighboring phenylene groups have no preferred angle between their planes. In conclusion, one can postulate that phenylene groups with proximate labeled carbons tend to have small angles between their $C_{ph}-O_{ph}$ directions but that the angle between their planes is random.

The qualitative discussion above can be put into a more quantitative framework. Let us consider the distribution function $P_{ph}(\alpha, \beta, \gamma, r)$ where $P_{ph}(\alpha, \beta, \gamma, r)\, d\alpha \sin(\beta)\, d\beta\, d\gamma\, dr$ is the probability to find two labeled phenylene carbons, whose distance is between r and $r + dr$, and whose CSA tensors have a relative orientation between Λ and $\Lambda + d\Lambda$; Λ represents the set of Euler angles (α, β, γ). The variations of the distance-integrated distribution $P_{ph}^{int}(\alpha, \beta, \gamma) = \int_0^\infty P_{ph}(\alpha, \beta, \gamma, r) r^{-6}\, dr$ are related to those of the distance factor. Therefore, information about $P_{ph}^{int}(\alpha, \beta, \gamma)$ can be obtained from the distance factor. However, a full fit of the three-dimensional distribution function is not possible. In the light of the above discussion, we restrict the dependence of the distribution function P_{ph}^{int} to a single parameter, β_{zz}, the angle between two $C_{ph}-O_{ph}$ directions. The distribution $P_{ph}^{int}(\beta_{zz})$ is assumed to be Gaussian and to have its maximum at $\beta_{zz} = 0°$. Using the principal values of the CSA tensors listed above, the half-width at half-height (hwhh) of $P_{ph}^{int}(\beta_{zz})$ was obtained from a least squares fit to the experimental distance factor. The fit included an overall scaling factor for the calculated values of f_d and an average over 30 different values of α and 30 different values of γ, both uniformly distributed. It yielded a hwhh of 77° ± 8°. The corresponding distribution is shown in Figure 4a, and the calculated distance factor in Figure 3c. The latter agrees well with that obtained experimentally (Figure 3b). From the ratio of the values of $P_{ph}^{int}(\beta_{zz})$ at 0° and 90°, ca. 2.3, the ratio of the mean distances between labeled carbons with parallel and perpendicular $C_{ph}-O_{ph}$ directions can be estimated. Since the distance factor scales as the inverse sixth power of the distance, the distance ratio is ca. 1.15.

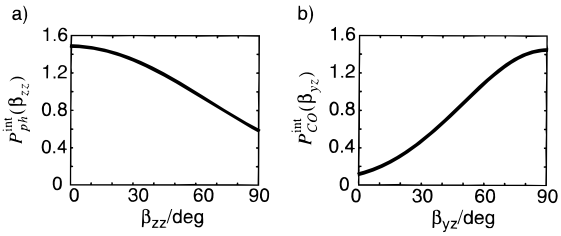

Figure 4. (a) Distance-integrated distribution function $P_{ph}^{int}(\beta_{zz})$ of the angle β_{zz} between two bonds connecting a phenylene ring to a carbonate group. The distribution was assumed to be Gaussian and centered at $\beta_{zz} = 0°$. Its width was obtained from a least squares fit to the distance factor of Figure 3b. The fit yielded a half-width at half-height of 77° ± 8° and the distance factor shown in Figure 3c. (b) Distance-integrated distribution function $P_{CO}^{int}(\beta_{yz})$ of the angle β_{yz} between the vector defined by the two ether oxygens of a carbonate group and the vector perpendicular to the plane of another carbonate group. The distribution was assumed to be Gaussian and centered at $\beta_{yz} = 90°$. Its width was obtained from a least squares fit to the distance factor of Figure 3e. The fit yielded a half-width at half-height of 47° ± 7° and the distance factor shown in Figure 3f.

The distance factor of the carbonate-labeled polymer is shown in Figure 3e. A maximum occurs in the region $\omega_A \approx \omega_B \approx \omega_{zz}$, which contains contributions from carbonate groups with nearly aligned $O_{ph}-O_{ph}$ directions. Since the torsional angle in the carbonate group is found almost exclusively in the trans conformation,[2,3] the $O_{ph}-O_{ph}$ direction can be associated with that of the polymer chain. In combination with the preference for small angles between the longitudinal axes of proximate phenylene groups, the high distance factor for carbonate groups with nearly aligned $O_{ph}-O_{ph}$ directions suggests that one tendency of the chains is to locally pack parallel. However, the distance factor of the carbonate groups does not follow the same trend as that of the phenylene groups. Along the line $\omega_A = \omega_{zz}$, f_d takes its minimal value at $\omega_B = \omega_{yy}$ and from there increases

when approaching $\omega_B = \omega_{xx}$. This behavior indicates that where two chain segments have close carbonate carbons, they do not simply tend to be parallel. They also adopt very different arrangements, where the $O_{ph}-O_{ph}$ direction of one carbonate group is parallel to the C=O direction of the other, so the two chain directions are perpendicular. Assuming that the distances between neighboring carbons in the parallel and perpendicular chain arrangements are the same, the probability of both arrangements, measured from the distance factor near (ω_{zz}, ω_{zz}) and at (ω_{zz}, ω_{xx}) in Figure 3e, are virtually equal. To the best of our knowledge, the occurrence of perpendicular chain segments has hitherto not been mentioned in the literature.

The distance factor in Figure 3e steadily increases when moving on the line $\omega_A = \omega_{yy}$ from the point $\omega_B = \omega_{zz}$ toward the diagonal. This variation can be explained by a distance-integrated distribution function $P_{CO}^{int}(\beta_{yz})$, in which the probability to find a small angle β_{yz}, between the *y* axis and the *z* axis of the CSA tensors of two neighboring carbonate carbons, is reduced compared to that at $\beta_{yz} = 90°$. Assuming $P_{CO}^{int}(\beta_{yz})$ to be a Gaussian function with its maximum at $\beta_{yz} = 90°$, the hwhh of the distribution was obtained from a least squares fit to the experimental distance factor. In the fit program, the two additional angles required to fully define the relative orientation of the CSA tensors were assumed to be uniformly distributed, and for each of them 30 different values were used. An overall scaling factor for the calculated distance factor was also included. The optimal rate factor is shown in Figure 3f and the distribution $P_{CO}^{int}(\beta_{yz})$ in Figure 4b. The hwhh of the distribution is 47° ± 8°. The simple model assumed here well reproduces the major variations of the experimental distance factor. However, since the spins that resonate at ω_{yy} do not necessarily have the *y* axis of their CSA tensor aligned with the magnetic field, an unambiguous interpretation of the variation of the distance factor along the line $\omega_A = \omega_{yy}$ is not possible.

4.III. Comparison with Atomistically Detailed Simulations. Knowing the orientation of the CSA tensors with respect to the local molecular frame, the calculation of distance factors according to eq 3 only involves distances between atoms and relative orientations between molecular fragments. Therefore, experimental distance factors as a function of the resonance frequencies ω_A and ω_B can easily be compared to factors calculated from atomistically detailed simulations.[30] The distance factors obtained from two different sets of atomistically detailed structures of polycarbonate are shown in Figure 5. The structures of both sets were generated according to the "amorphous cell" algorithm[30] followed by a molecular dynamics "annealing" procedure using the unconstrained Cartesian-coordinate force field pcff91.[31] The size of the simulation box of the first set[32] is 29.78 Å (Figure 5a,b) and that of the second set[33] is 20.13 Å (Figure 5c,d).

The calculated distance factors for the phenylene-labeled polymer, shown in Figure 5a,c, are highest in the region where $\omega_A \approx \omega_B \approx \omega_{xx}$. In this region, pairs of phenylene groups with nearly parallel aromatic planes contribute to the distance factor. Along the line $\omega_A = \omega_{zz}$, f_d increases between ω_{xx} and ω_{yy}, but is constant elsewhere. These variations suggest that close packing of the nearly coplanar phenylene groups predominates in the simulated structures. This is in contradiction with the conclusion drawn from the experimental distance factor, namely that the angle between neighboring phenylene planes is random. The simulations are static structures near their potential-energy minima which do not account for the large amplitude oscillations of the phenylene groups at room temperature.[25−28] This deficiency could explain the preference for small angles between the phenylene planes in the simulated structures.

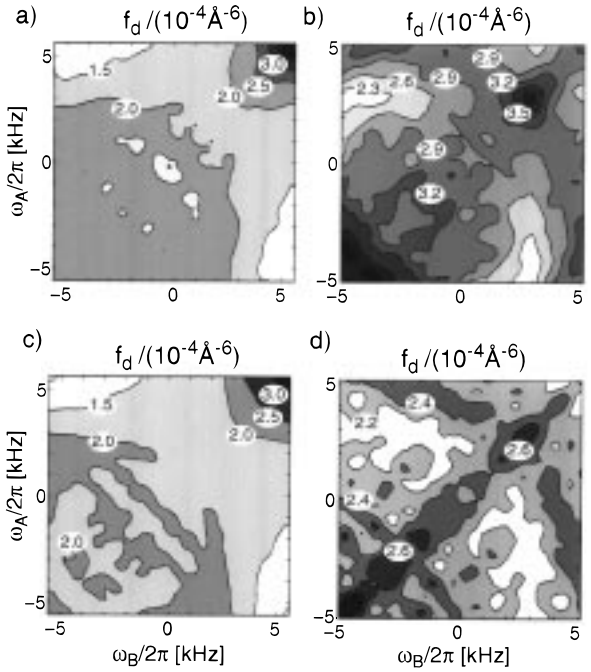

Figure 5. Distance factors as a function of the resonance frequencies ω_A and ω_B calculated from atomistically detailed structures of bisphenol-A polycarbonate using the orientations of the chemical-shielding-anisotropy tensors shown in Figure 2. Distance factors of (a) the phenylene-labeled polycarbonate and (b) the carbonate-labeled polycarbonate obtained from an average over a set of five structures. Each structure has a degree of polymerization $x = 150$ ($M = 19014$) and is contained in a box of edge length 29.78 Å. Distance factors of (c) the phenylene-labeled polycarbonate and (d) the carbonate-labeled polycarbonate obtained from an average over a set of nine structures. Each structure has a degree of polymerization $x = 46$ ($M = 5956$) and is contained in a box of edge length 20.13 Å.

The calculated distance factors for the carbonate groups are shown in Figure 5b,d. Both sets of data contain a valley along the line $\omega_A = \omega_{yy}$. The valley is more pronounced in the factor calculated from the structure with the larger box-edge length (Figure 5b). Except for an overall scaling factor, this data set agrees well with the experimental data in Figure 3e. Inspection of the atomistic structures reveals a wide distribution of the relative orientation between the carbonate groups, with parallel and perpendicular chain segments. The lowered distance factor in the region $\omega_A \approx \omega_{yy}$, $\omega_B \approx \omega_{zz}$ is due to a larger distance between the carbons in arrangements where the $O_{ph}-O_{ph}$ direction of one group is perpendicular to the carbonate plane of the other. This distance difference is caused by sterical hindrance.

In general, the calculated distance factors are larger than those obtained experimentally. This difference might have several origins. Deviations from the initial rate regime, where off-diagonal intensities are assumed to increase linearly with the mixing time, lead to reduced experimental distance factors.[20] However, this

effect is very unlikely to account for the full difference. The absence of molecular motion or the occurrence of a wider distance distribution in the simulated structures could explain the larger values of the distance factors calculated from the simulations.

4.IV. Compatability of the Experimental Distance Factors with the "Bundle" Model. In the "bundle" model[6−10] the polymer chains adopt an extended conformation and are locally packed parallel to each other (see Figure 6 in ref 9). The model includes a unspecified degree of orientational disorder to account for the amorphous nature of the packing. Such a model with locally parallel chains consists of nearest neighbor phenylene groups with approximately parallel $C_{ph}-O_{ph}$ directions and nearest neighbor carbonate groups with approximately parallel $O_{ph}-O_{ph}$ directions. These arrangements lead, for both labeled polymers used in this study, to maximal distance factors in the region where $\omega_A \approx \omega_B \approx \omega_{zz}$ and to strongly reduced values at $(\omega_A, \omega_B) = (\omega_{xx}, \omega_{zz})$. This tendency is observed for the distance factor of the phenylene-labeled polymer in Figure 3b. However, the distance factor of the carbonate-labeled polymer (Figure 3e) takes high values not only in the region predicted by the "bundle" model but also where contributions arise from chains which are perpendicular to each other. This additional characteristic of the packing of the carbonate groups is diametrically opposed to the "bundle" model.

The "bundle" model was inferred from a set of experimental data interpreted in the light of the structures of analogous low molecular weight compounds[23] and of crystalline polycarbonate,[34] which contain parallel chains. None of the experimental techniques used[4−9] directly probed local orientational order between different chain segments. Therefore, it is not surprising that the presence of neighboring perpendicular chain segments was not accounted for.

5. Conclusion

The local orientational order between phenylene groups and between carbonate groups in glassy bisphenol-A polycarbonate has been investigated using two-dimensional S-MAS polarization-transfer NMR spectroscopy. This technique is directly sensitive to the relative orientation of neighboring groups. The distance dependence of the polarization-transfer rate constant measured as a function of the resonance frequencies can be easily isolated and interpreted in terms of preferred orientations between molecular groups. However, because of the equivocal relation between resonance frequency and CSA orientation, extraction of angular distributions is limited. This problem might be alleviated by using more elaborated measurement techniques in which the resonance frequencies are sampled at several rotor positions.

The local order between phenylene groups in polycarbonate is characterized by a preference for small angles between their longitudinal axes, while the relative orientation between the radial directions seems random. These features were not found in atomistically detailed simulations of glassy polycarbonate. This shortcoming of the simulations considered herein might originate from the limited size of simulated structures or from neglecting molecular motion in the simulations. For carbonate groups, two closely packed arrangements dominate: either the two vectors defined by the pairs of ether oxygens in each group make a small angle or one of these vectors is nearly aligned with the C═O double bond of the other group. This tendency was also found in atomistically detailed simulations of glassy polycarbonate.

This existence of closely packed carbonate groups with perpendicular directions defined by the pairs of ether oxygens in each group is the most striking structural characteristic exposed in this work. Such arrangements are not contained in the "bundle" model[6−9] for glassy polycarbonate, according to which the extended polymer chains are locally packed parallel to each other. These arrangements decisively augment the complexity of model structures of glassy polycarbonate. They are possibly related to the weak crystallization tendency of this polymer.[34]

Acknowledgment. This work was supported by the Swiss National Science Foundation. We thank Dr. Marcel Utz for valuable discussions, Dr. Marcel Zehnder for his help with the atomistic simulations, and Prof. Richard R. Ernst for his support and guidance.

References and Notes

(1) Henrichs, P. M.; Nicely, V. A. *Macromolecules* **1990**, *23*, 3193−3194.
(2) Tomaselli, M.; Robyr, P.; Meier, B. H.; Grob-Pisano, C.; Ernst, R. R.; Suter, U. W. *Mol. Phys.* **1996**, *89*, 1663−1694.
(3) Tomaselli, M.; Zehnder, M. M.; Robyr, P.; Grob-Pisano, C.; Ernst, R. R.; Suter, U. W. *Macromolecules* **1997**, *30*, 3579−3583.
(4) Cervinka, L.; Fischer, E. W.; Hahn, K.; Jiang, B.-Z.; Hellmann, G. P.; Kuhn, K.-J. *Polymer* **1987**, *28*, 1287−1292.
(5) Cervinka, L.; Fischer, E. W.; Dettenmaier, M. *Polymer* **1991**, *32*, 12−18.
(6) Schmidt, A.; Kowalewski, T.; Schaefer, J. *Macromolecules* **1993**, *26*, 1729−1733.
(7) Lee, P. L.; Schaefer, J. *Macromolecules* **1995**, *28*, 1921−1924.
(8) Lee, P. L.; Kowalewski, T.; Poliks, M. D.; Schaefer, J. *Macromolecules* **1995**, *28*, 2476−2482.
(9) Klug, C. A.; Zhu, W.; Tasaki, K.; Schaefer, J. *Macromolecules* **1997**, *30*, 1734−1740.
(10) Duane, R. W.; Yaris, R. *Macromolecules* **1997**, *30*, 1741−1751.
(11) Lamers, C.; Schönfield, C.; Shapiro, S. M.; Batoulis, J.; Timmermann, R.; Cable, J. W.; Richter, D. *Colloid Polym. Sci.* **1994**, *272*, 1403−1419.
(12) Robyr, P.; Tomaselli, M.; Straka, J.; Grob-Pisano, C.; Suter, U. W.; Meier, B. H.; Ernst, R. R. *Mol. Phys.* **1995**, *84*, 995−1020. Robyr, P.; Tomaselli, M.; Grob-Pisano, C.; Meier, B. H.; Ernst, R. R.; Suter, U. W. *Macromolecules* **1995**, *28*, 5320−5324.
(13) Abragam, A. The Principles of Nuclear Magnetism; Clarendon: Oxford, 1961.
(14) Suter, D.; Ernst, R. R. *Phys. Rev. B* **1985**, *32*, 5608−5627.
(15) Mehring, M. *High Resolution NMR in Solids*; Springer: Heidelberg, 1983.
(16) Veeman, W. S. *Prog. Nucl. Magn. Reson. Spectrosc.* **1984**, *16*, 193−235.
(17) Robyr, P.; Meier, B. H.; Ernst, R. R. *Chem. Phys. Lett.* **1989**, *162*, 417−423.
(18) Meier, B. H. *Adv. Magn. Opt. Reson.* **1994**, *18*, 1−116.
(19) Gan, Z.; Ernst, R. R. *Chem. Phys. Lett.* **1996**, *253*, 13−19.
(20) Robyr, P.; Gan, Z. *J. Magn. Reson.* **1998**, *131*, 254−260.
(21) Ernst, R. R.; Bodenhausen, G.; Wokaun, A. *Principles of Nuclear Magnetic Resonance in One and Two Dimensions*; Clarendon: Oxford, 1987.
(22) Hester, R. K.; Ackerman, J. L.; Neff, B. L.; Waugh, J. S. *Phys. Rev. Lett.* **1976**, *36*, 1081−1083. Rybaczewski, E. F.; Neff, B. L.; Waugh, J. S.; Sherfinski, J. S. *J. Chem. Phys.* **1977**, *67*, 1231−1235.
(23) Perez, S.; Scaringe, R. P. *Macromolecules* **1987**, *20*, 68−77.
(24) Robyr, P.; Utz, M.; Gan, Z.; Scheurer, C.; Tomaselli, M.; Suter, U. W.; Ernst, R. R. *Macromolecules* (in press).
(25) Spiess, A. W. *Colloid Polym. Sci.* **1983**, *261*, 193−209.
(26) Schaefer, J.; Stejskal, E. O.; Perchak, D.; Skolnick, J.; Yaris, R. *Macromolecules* **1985**, *18*, 368−373.
(27) Jones, A. A. *Macromolecules* **1985**, *18*, 902−906.

(28) Roy, A. K.; Jones, A. A.; Inglfield, P. T. *Macromolecules* **1986**, *19*, 1356−1362.
(29) Henrichs, P. M.; Linder, M.; Hewitt, J. M.; Massa, D.; Isaacson, H. V. *Macromolecules* **1984**, *17*, 2412−2416.
(30) Theodorou, D. N.; Suter, U. W. *Macromolecules* **1985**, *18*, 1457−1478.
(31) Maple, J. R.; Hwang, M.-J.; Stockfisch, T. P.; Dinur, U.; Waldman, M.; Ewig, C. S.; Hagler, A. T. *J. Comput. Chem.* **1994**, *15*, 162−182.
(32) Tiller, A.; Gusev, A. A.; Suter, U. W. (in preparation).
(33) Tschöp, W.; Kremer, K.; Batoulis, J.; Bürger, T.; Hahn, O. *Acta Polym.* **1998**, *49*, 61−74.
(34) Bonart, A. *Makromol. Chem.* **1966**, *92*, 149−169.

MA980447G